

See discussions, stats, and author profiles for this publication at: <https://www.researchgate.net/publication/238649785>

Monochlorogallane: Physical Properties and Structure of the Gaseous Molecule $\text{H}_2\text{Ga}(\mu\text{-Cl})_2$ GaH_2 As Determined by Vibrational, Electron Diffraction, and ab Initio Studies

ARTICLE in INORGANIC CHEMISTRY · FEBRUARY 2000

Impact Factor: 4.76 · DOI: 10.1021/ic9908975

CITATIONS

22

READS

18

11 AUTHORS, INCLUDING:



Anthony J Downs

University of Oxford

258 PUBLICATIONS 5,200 CITATIONS

SEE PROFILE



Kirsten Aarset

Oslo and Akershus University College of Appl...

31 PUBLICATIONS 251 CITATIONS

SEE PROFILE



David A. Rice

University of Reading

145 PUBLICATIONS 1,730 CITATIONS

SEE PROFILE



Colin Pulham

The University of Edinburgh

140 PUBLICATIONS 2,316 CITATIONS

SEE PROFILE

Monochlorogallane: Physical Properties and Structure of the Gaseous Molecule $\text{H}_2\text{Ga}(\mu\text{-Cl})_2\text{GaH}_2$ As Determined by Vibrational, Electron Diffraction, and *ab Initio* Studies

Emma Johnsen, Anthony J. Downs,* Timothy M. Greene, and Philip F. Souter

Inorganic Chemistry Laboratory, University of Oxford, South Parks Road, Oxford OX1 3QR, U.K.

Kirsten Aarset, Elizabeth M. Page, and David A. Rice

Department of Chemistry, University of Reading, Whiteknights, P.O. Box 224, Reading RG6 6AD, U.K.

Alan N. Richardson

Department of Chemistry, Oregon State University, Corvallis, Oregon 97331-4003

Paul T. Brain, David W. H. Rankin, and Colin R. Pulham

Department of Chemistry, University of Edinburgh, West Mains Road, Edinburgh EH9 3JJ, U.K.

Received July 28, 1999

Monochlorogallane, synthesized by the metathesis of gallium(III) chloride with an excess of trimethylsilane at ca. 250 K, has been characterized by chemical analysis, by its IR, Raman, and ^1H NMR spectra, and by the products of its reaction with trimethylamine. The vibrational spectra of the vapor species isolated in solid Ar, N_2 , or CH_4 matrixes at ca. 12 K imply the presence of only one species, viz. the dimer with an equilibrium structure conforming to D_{2h} symmetry. The structure of this molecule has been determined by gas-phase electron diffraction (GED) measurements augmented by the results of *ab initio* molecular orbital calculations. An equilibrium structure with D_{2h} symmetry has been assumed in the analysis of the electron diffraction pattern. However, as the molecule has a very low frequency $\text{Ga}(\mu\text{-Cl})_2\text{Ga}$ ring-puckering mode, a dynamic model was used to describe it with the aid of a set of pseudoconformers spaced at even intervals ($\Delta\delta = 5^\circ$, $\delta_{\text{max}} = 20^\circ$) around the ring-puckering angle δ and Boltzmann-weighted according to a quartic potential $V(\delta) = V_4\delta^4 + V_2\delta^2$. The differences in bond distances and angles between the different pseudoconformers were constrained to the values derived from the *ab initio* calculations employing second-order Møller–Plesset (MP2) methods (with all the electrons included in the correlation calculations) and a 6-311G(d) basis set. The results for the weighted average of the principal distances (r_α) and angles (\angle_α) (with estimated 1σ uncertainties) from the combined GED/*ab initio* study are $r(\text{Ga}-\text{Cl})$ 2.350(2) Å, $r(\text{Ga}-\text{H})$ 1.523(20) Å, $\angle\text{Cl}-\text{Ga}-\text{Cl}$ 89.7(5)°, $\angle\text{H}-\text{Ga}-\text{H}$ 135.1°, V_4 3.0×10^{-6} kcal mol $^{-1}$ deg $^{-4}$, and V_2 6.0×10^{-4} kcal mol $^{-1}$ deg $^{-2}$.

Introduction

The renaissance of interest in hydrides of aluminum and gallium owes much to their potential applications in chemical vapor deposition technology and related materials science^{1–4} and in chemical synthesis.⁵ Up to the present, monosubstituted derivatives of gallane of the type GaH_2X have remained comparatively elusive. Stabilization of the intrinsically rather

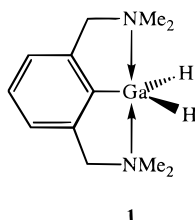
fragile GaH_2 unit may be achieved through coordination to a suitable Lewis base (e.g., Me_3N or quinuclidine⁶) or with the aid of bridging ligands to give cyclic compounds of the type $[\text{H}_2\text{Ga}(\mu\text{-X})]_n$ ($n = 2, 3$; $\text{X} = \text{NH}_2$,⁴ NMe_2 ,⁷ NEt_2 ,⁸ $\text{P}(\text{cyclohexyl})_2$,⁹ OBu^t ,¹⁰ or OCHBu^t ¹¹). Compounds where X is an

* Corresponding author. Tel: 0044 (1865) 272673. Fax: 0044 (1865) 272690. E-mail: tony.downs@chem.ox.ac.uk.

- (1) Taylor, M. J.; Brothers, P. J. In *Chemistry of Aluminium, Gallium, Indium and Thallium*; Downs, A. J., Ed.; Blackie: Glasgow, U.K., 1993; pp 111–247.
- (2) Downs, A. J.; Pulham, C. R. *Adv. Inorg. Chem.* **1994**, *41*, 171; *Chem. Soc. Rev.* **1994**, *23*, 175. Downs, A. J. *Coord. Chem. Rev.* **1999**, *189*, 59.
- (3) Jones, C.; Koutsantonis, G. A.; Raston, C. L. *Polyhedron* **1993**, *12*, 1829. Raston, C. L. *J. Organomet. Chem.* **1994**, *475*, 15. Gardiner, M. G.; Raston, C. L. *Coord. Chem. Rev.* **1997**, *166*, 1.
- (4) Campbell, J. P.; Hwang, J.-W.; Young, V. G., Jr.; Von Dreele, R. B.; Cramer, C. J.; Gladfelter, W. L. *J. Am. Chem. Soc.* **1998**, *120*, 521 and references therein.

- (5) See, for example: Henderson, M. J.; Kennard, C. H. L.; Raston, C. L.; Smith, G. J. *Chem. Soc., Chem. Commun.* **1990**, 1203. Atwood, J. L.; Bott, S. G.; Jones, C.; Raston, C. L. *Inorg. Chem.* **1991**, *30*, 4868.
- (6) Greenwood, N. N. In *New Pathways in Inorganic Chemistry*; Ebsworth, E. A. V., Maddock, A. G., Sharpe, A. G., Eds.; Cambridge University Press: Cambridge, U.K., 1968; pp 37–64. Luo, B.; Young, V. G., Jr.; Gladfelter, W. L. *J. Chem. Soc., Chem. Commun.* **1999**, 123.
- (7) Baxter, P. L.; Downs, A. J.; Rankin, D. W. H.; Robertson, H. E. *J. Chem. Soc., Dalton Trans.* **1985**, 807.
- (8) Lorberth, J.; Dorn, R.; Massa, W.; Wocadlo, S. Z. *Naturforsch., B* **1993**, *48*, 224.
- (9) Elms, F. M.; Koutsantonis, G. A.; Raston, C. L. *J. Chem. Soc., Chem. Commun.* **1995**, 1669.
- (10) Veith, M.; Faber, S.; Wolfanger, H.; Huch, V. *Chem. Ber.* **1996**, *129*, 381.
- (11) Koutsantonis, G. A.; Lee, F. C.; Raston, C. L. *Main Group Chem.* **1995**, *1*, 21.

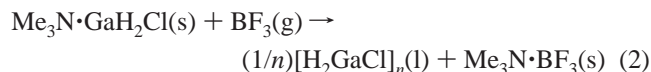
organic group, e.g. $X = \text{Et}$,¹² are typically labile at ambient temperatures unless X is very bulky [as in the case of the monomeric species (2,4,6- $\text{Bu}^t_3\text{C}_6\text{H}_2$) GaH_2] or carries basic substituents (as in **1**).¹³



Lewis base-free monosubstituted derivatives of gallane tend otherwise to resemble gallane itself^{12,14} in being short-lived at ambient temperatures, as is the case, for example, with $[\text{H}_2\text{GaBH}_4]_n$ ^{15,16} and $\text{H}_2\text{GaB}_3\text{H}_8$.¹⁷ The monomeric molecule H_2GaCl is formed by the photoinduced addition of H_2 to molecular GaCl isolated in a solid argon matrix (eq 1).¹⁸ Earlier



studies had suggested¹⁹ that monochlorogallane is displaced as an oil from the adduct $\text{Me}_3\text{N} \cdot \text{GaH}_2\text{Cl}$ by the action of BF_3 in accordance with eq 2, although the product, said to decompose



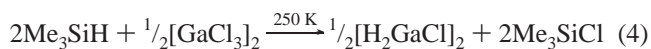
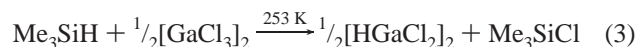
rapidly below room temperature, eluded detailed characterization. On the other hand, subsequent studies^{20a-c} of the analogous reaction between $\text{Me}_3\text{N} \cdot \text{GaH}_3$ and BF_3 disclose that the predominant pathway entails not displacement^{20d} but halide-hydride exchange. Accordingly, there must be serious reservations about the earlier claims to have made not only gallane itself^{20d} but also monochlorogallane.¹⁹

Here we report the synthesis and some of the physical properties of monochlorogallane, a labile liquid at ambient temperatures. On the evidence of its vibrational spectra and electron diffraction pattern, the vapor consists predominantly of the dimeric molecules $\text{H}_2\text{Ga}(\mu\text{-Cl})_2\text{GaH}_2$, the structure of which has been determined both by experiment and by ab initio calculations. A subsequent paper will describe some of the chemical properties of the compound.²¹ A preliminary account of some of these studies has appeared previously,²² and the

vibrational spectra of monochlorogallane have also been analyzed in some detail.²³

Results and Discussion

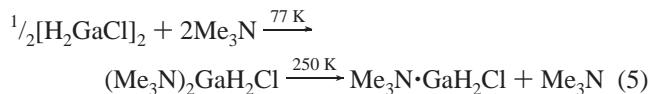
(a) Synthesis and Validation. That dichlorogallane, $[\text{HGaCl}_2]_2$, is produced by chloride-hydride metathesis between gallium(III) chloride and trimethylsilane (eq 3) is established beyond doubt.²⁴ We have found that trimethylsilane in 5–10-fold excess reacts efficiently with powdered gallium(III) chloride under solvent-free conditions at ca. 250 K in accordance with eq 4 to



give monochlorogallane. The compound can be isolated by fractional condensation in vacuo of the volatile material, being retained by a trap cooled to 228 K. Fractionation gives a homogeneous product judged to be essentially pure monochlorogallane, typically in yields of 80% or better based on the quantity of gallium(III) chloride taken and consumed in accordance with eq 4. Vaporization typically gives rise to slight decomposition, yielding both more volatile and less volatile products, the nature of which will be discussed later. The successful synthesis of monochlorogallane demands the use of scrupulously pure reagents and rigorous exclusion of moisture, grease, or other contaminants; this has necessitated the development of appropriate vacuum-line procedures, with pressures $<10^{-4}$ mmHg, short distillation paths, minimal use even of greaseless valves, and preconditioning of all glassware (by heating under continuous pumping).^{2,14}

Monochlorogallane condenses at low temperatures, usually as a colorless glass that softens at about 213 K to give a very viscous oil. Attempts to grow crystals have met with no success. The viscosity of the liquid decreases markedly as the temperature is raised, and at temperatures >293 K, the compound exists as a mobile liquid. The rate of vaporization is consistent with a vapor pressure of 0.1–0.5 mmHg at 293 K. A sample of the liquid sealed in vacuo in a rigorously preconditioned glass ampule shows significant signs of decomposition only after a day or so at room temperature.

As reported briefly elsewhere,²² monochlorogallane has been authenticated chemically by quantitative chemical assay of its decomposition products and by trapping with trimethylamine followed by spectroscopic identification of the resulting products (see eq 5). Its identity and likely structure have been endorsed



by its IR and Raman and ^1H NMR spectra. The spectroscopic results argue for a dimeric molecule $\text{H}_2\text{Ga}(\mu\text{-Cl})_2\text{GaH}_2$ with D_{2h} symmetry as the predominant species in the vapor phase, although there is evidence of significant intermolecular interactions and probably of further aggregation in the liquid and solid states. The postulation of a dimeric structure is supported by

(12) Grady, A. S.; Markwell, R. D.; Russell, D. K. *J. Chem. Soc., Chem. Commun.* **1991**, 14.

(13) Cowley, A. H.; Gabbai, F. P.; Isom, H. S.; Decken, A. J. *Organomet. Chem.* **1995**, 500, 81.

(14) Pulham, C. R.; Downs, A. J.; Goode, M. J.; Rankin, D. W. H.; Robertson, H. E. *J. Am. Chem. Soc.* **1991**, 113, 5149.

(15) Pulham, C. R.; Brain, P. T.; Downs, A. J.; Rankin, D. W. H.; Robertson, H. E. *J. Chem. Soc., Chem. Commun.* **1990**, 177.

(16) Downs, A. J.; Parsons, S.; Pulham, C. R.; Souter, P. F. *Angew. Chem., Int. Ed. Engl.* **1997**, 36, 890.

(17) Pulham, C. R.; Downs, A. J.; Rankin, D. W. H.; Robertson, H. E. *J. Chem. Soc., Dalton Trans.* **1992**, 1509. Morrison, C. A.; Smart, B. A.; Brain, P. T.; Pulham, C. R.; Rankin, D. W. H.; Downs, A. J. *J. Chem. Soc., Dalton Trans.* **1998**, 2147.

(18) Köppe, R.; Schnöckel, H. *J. Chem. Soc., Dalton Trans.* **1992**, 3393.

(19) Greenwood, N. N.; Storr, A. *J. Chem. Soc.* **1965**, 3426.

(20) (a) Shirk, A. E.; Shirk, J. S. *Inorg. Chem.* **1983**, 22, 72. (b) Baxter, P. L. D. Philos. Thesis, University of Oxford, U.K., 1984. (c) Goode, M. J. D. Philos. Thesis, University of Oxford, U.K., 1987. (d) Greenwood, N. N.; Wallbridge, M. G. H. *J. Chem. Soc.* **1963**, 3912.

(21) Johnsen, E.; Downs, A. J.; Goode, M. J.; Greene, T. M.; Müller, M.; Parsons, S.; Pulham, C. R. In preparation.

(22) Goode, M. J.; Downs, A. J.; Pulham, C. R.; Rankin, D. W. H.; Robertson, H. E. *J. Chem. Soc., Chem. Commun.* **1988**, 768.

(23) Pulham, C. R.; Downs, A. J.; Goode, M. J.; Greene, T. M.; Mills, I. M. *Spectrochim. Acta, Part A* **1995**, 51, 769.

(24) Schmidbaur, H.; Findeiss, W.; Gast, E. *Angew. Chem., Int. Ed. Engl.* **1965**, 4, 152. Schmidbaur, H.; Klein, H.-F. *Chem. Ber.* **1967**, 100, 1129.

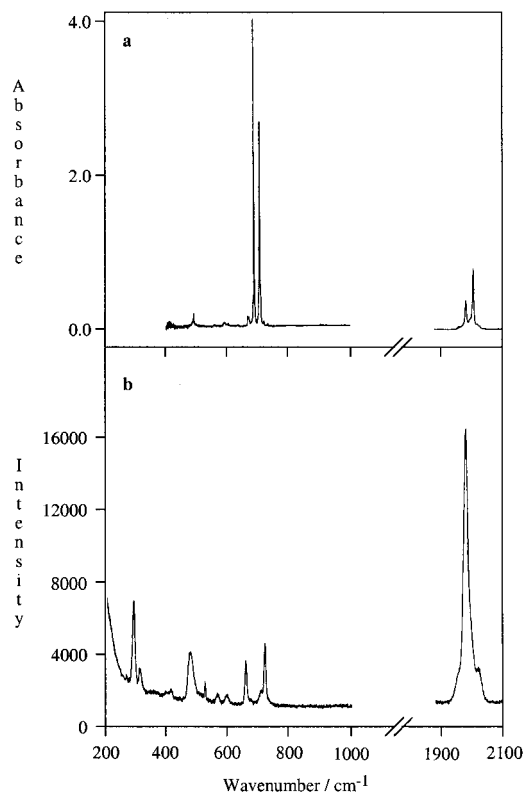


Figure 1. (a) IR and (b) Raman spectra of $\text{H}_2\text{Ga}(\mu\text{-Cl})_2\text{GaH}_2$ molecules isolated in a methane matrix at ca. 20 K.

an analysis of the gas-phase electron diffraction data of the vapor at ca. 320 K and by the results of ab initio calculations.

(b) Vibrational Spectra of Monochlorogallane. The low vapor pressure and thermal instability of monochlorogallane negate direct measurements of the IR spectrum of the vapor; instead we have had to trap the vapor molecules in solid matrixes at low temperatures. As already reported,²³ the IR spectrum of such a matrix containing either [$^1\text{H}_4$]- or [$^2\text{H}_4$]monochlorogallane implies the presence of dimeric molecules $\text{H}_2\text{Ga}(\mu\text{-Cl})_2\text{GaH}_2$ with D_{2h} symmetry; it is also similar to the spectrum of a solid film of the compound. Under D_{2h} symmetry, the 18 vibrational fundamentals of the dimer span the representation $4a_g + 1a_u + 2b_{2g} + 3b_{2u} + 2b_{1g} + 2b_{1u} + 1b_{3g} + 3b_{3u}$ (where the choice of x , y , and z axes follows the convention of Duncan et al. in their definitive analysis of the vibrational spectra of diborane²⁵). The fundamentals are thus mutually exclusive with regard to Raman activity ($4a_g + 2b_{2g} + 2b_{1g} + 1b_{3g}$) and IR activity ($3b_{2u} + 2b_{1u} + 3b_{3u}$), with the unique a_u mode being inactive in both spectra. In an earlier analysis, information about the Raman-active modes was drawn from the spectrum of the liquid at 213 K on the assumption that the liquid is composed of the same dimeric molecules more or less unperturbed by intermolecular forces. We have now succeeded in measuring the Raman spectrum of [$^1\text{H}_4$]- and [$^2\text{H}_4$]monochlorogallane vapor isolated in a solid argon, nitrogen, or methane matrix at ca. 20 K. Typical Raman and IR spectra of matrix-isolated samples are illustrated in Figure 1; details of the relevant frequencies and intensities are given in Tables 1 and 2. Included in the tables are the harmonic frequencies and intensities forecast by ab initio quantum chemical calculations.

The matrix spectra have been interpreted on the basis of four main criteria: (a) the selection rules expected to govern the

activity of modes in IR absorption and Raman scattering; (b) the effect of deuteration on the position of a given transition in the vibrational spectrum; (c) comparisons with the spectra of related molecules, e.g. Ga_2Cl_6 ²⁶ and Ga_2H_6 ,¹⁴ and (d) comparisons with the results of the ab initio calculations [at the Hartree–Fock (HF) level of theory and with a 6-311G(d) basis set]. There are some complications due to matrix site splittings, notably in the spectra of argon and nitrogen matrixes; contamination is liable also to be a problem with a compound as reactive and thermally frail as monochlorogallane, and the perdeuterated sample was certainly contaminated with small amounts of incompletely deuterated isotopomers such as $\text{HDGa}(\mu\text{-Cl})_2\text{GaD}_2$. However, the principal features of the spectra agree satisfactorily with the calculated properties; only in the low-frequency region of the Raman spectra do overtone and combination bands introduce some additional problems of interpretation.

The Raman spectra of the matrix samples contain seven of the nine Raman-active fundamentals, namely ν_1 , ν_2 , ν_3 , ν_6 , ν_{11} , ν_{12} , and ν_{15} and, through combination and overtone bands, appear also to give indirect access to approximate frequencies for the remaining two, namely ν_4 and ν_7 , both of which are predicted to be very weak in Raman scattering. All the frequencies quoted hereafter relate to argon matrixes, the values given in parentheses referring to the perdeuterated molecule [D_2GaCl]₂. The prominent bands appearing at 2036 (1458) and 1994 (1429) cm^{-1} are clearly associated with the $\nu(\text{Ga-H})$ modes ν_{11} and ν_1 , respectively. In order of decreasing frequency, the next scattering to appear is at 719 (515) cm^{-1} , which can be confidently assigned to the symmetric GaH_2 scissoring mode ν_2 , whereas the neighboring feature at 656 (476) cm^{-1} is most plausibly attributed to the out-of-phase GaH_2 wagging mode ν_6 . A broad band centered near 475 (350) cm^{-1} appears to take in the out-of-plane GaH_2 rocking and GaH_2 torsion modes, i.e. ν_{12} and ν_{15} , respectively. As the relatively strong emission at 292 cm^{-1} exhibits no perceptible change of frequency on deuteration, it is plainly associated with the symmetric $\nu(\text{Ga-Cl})$ mode ν_3 . This leaves four weak bands at 593 (431), 412 (410), 311 (311), and 268 (267) cm^{-1} ; on the evidence of their frequencies and intensities, none of these is an obvious candidate for a fundamental transition. The feature at highest frequency we attribute to the combination $\nu_4 + \nu_{12}$ (B_{1g}) or $\nu_4 + \nu_{15}$ (B_{3g}). The bands near 412, 311, and 268 cm^{-1} can be associated with the combination $\nu_3 + \nu_4$ (A_g), the combination $\nu_4 + \nu_7$ (B_{2g}), and the overtone $2\nu_4$ (A_g), respectively; in no case is deuteration expected to produce more than a slight change of frequency in any of these. These proposals imply a frequency near 130 cm^{-1} for ν_4 , in good agreement with the calculated harmonic value. It then follows that ν_7 occurs near 180 cm^{-1} , compared with the calculated value of 145 cm^{-1} . Weak scattering at 523 cm^{-1} in the spectrum of [H_2GaCl]₂, which has no obvious counterpart in the spectrum of [D_2GaCl]₂, could be due to a trace of impurity (e.g., [HGaCl_2]₂²⁴) or conceivably the overtone $2\nu_{18}$ (A_g).

Most of the other fundamentals can be identified on the basis of the IR spectra of the matrix-isolated species, but two have so far escaped detection. These are ν_5 (a_u), one of the GaH_2 torsions which is inactive in IR absorption and Raman scattering, and ν_{10} (b_{2u}), the IR-active ring-puckering motion which is expected to occur at $\tilde{\nu} < 40$ cm^{-1} , i.e. outside the limits of the experimental measurements made to date. Under the circumstances, we have had to rely on the results of the ab initio calculations to set the wavenumbers of these modes.

(25) Duncan, J. L.; Harper, J.; Hamilton, E.; Nivellini, G. D. *J. Mol. Spectrosc.* **1983**, 102, 416.

(26) Beattie, I. R.; Gilson, T.; Cocking, P. *J. Chem. Soc. A* **1967**, 702. Sjøgren, C. E.; Klæboe, P.; Rytter, E. *Spectrochim. Acta, Part A* **1984**, 40, 457.

Table 1. Observed and Calculated Frequencies (cm^{-1}) and Intensities of the Vibrational Fundamentals of the $[\text{H}_2\text{GaCl}]_2$ Molecule^a

mode	obsd freq	calcd freq	calcd freq ^b	obsd activity ^c		predicted activity	
				IR	Raman	IR	Raman
ν_1 (a_g)	1994, ^d 1999, ^e 1994 ^f	2105.8	1997.7	0	100	0.0	100.0
ν_2 (a_g)	719, ^d 721, ^e 721 ^f	763.9	724.7	0	10	0.0	5.3
ν_3 (a_g)	291, ^d 291, ^e 292 ^f	286.0	271.3	0	20	0.0	1.3
ν_4 (a_g)	ca. 130 ^g	147.4	139.9	0	0	0.0	0.3
ν_5 (a_u)		465.8	441.9	0	0	0.0	0.0
ν_6 (b_{2g})	656, ^d 660, ^e 656 ^f	683.8	648.7	0	7	0.0	4.0
ν_7 (b_{2g})	ca. 180 ^h	152.4	144.6	0	0	0.0	0.04
ν_8 (b_{2u})	2021, ^d 2026, ^e 2000 ^f	2107.9	1999.7	50	0	86.1	0.0
ν_9 (b_{2u})	480, ^d 492, ^e 492 ^f	503.8	478.0	5	0	16.0	0.0
ν_{10} (b_{2u})		35.9	34.1			0.2	0.0
ν_{11} (b_{1g})	2036, ^d 2042, ^e 2030 ^f	2104.9	1996.9	0	15	0.0	28.5
ν_{12} (b_{1g})	477, ^d 486, ^e 471 ^f	480.8	456.1	0	<1	0.0	1.9
ν_{13} (b_{1u})	702, ^d 706, ^e 685 ^f	730.1	692.6	70	0	80.3	0.0
ν_{14} (b_{1u})	290 ^d	258.4	245.1	15	0	15.1	0.0
ν_{15} (b_{3g})	472, ^d 475, ^e 467 ^f	466.2	442.2	0	20	0.0	4.9
ν_{16} (b_{3u})	1998, ^d 2004, ^e 1980 ^f	2101.7	1993.8	25	0	34.5	0.0
ν_{17} (b_{3u})	702, ^d 693, ^e 704 ^f	747.5	709.1	100	0	100.0	0.0
ν_{18} (b_{3u})	265 ^d	262.3	248.8	20	0	36.5	0.0

^a Observed spectra relate to the matrix-isolated molecule. Calculated frequencies and relative intensities (estimated relative to the strongest band set to 100 arbitrary units) were obtained using HF/6-311G(d). ^b Corresponding force constants scaled by 0.9. ^c Observed intensities estimated relative to the strongest band set to 100 arbitrary units. ^d Argon matrix. ^e Dinitrogen matrix. ^f Methane matrix. ^g Inferred from $2\nu_4$ at 268 cm^{-1} and ($\nu_3 + \nu_4$) at 412 cm^{-1} . ^h Inferred from ($\nu_4 + \nu_7$) at 311 cm^{-1} .

Table 2. Observed and Calculated Frequencies (cm^{-1}) and Intensities of the Vibrational Fundamentals of the $[\text{D}_2\text{GaCl}]_2$ Molecule^a

mode	obsd freq	calcd freq	calcd freq ^b	obsd activity ^c		predicted activity	
				IR	Raman	IR	Raman
ν_1 (a_g)	1429, ^d 1433, ^e 1430 ^f	1492.2	1415.6	0	100	0.0	100.0
ν_2 (a_g)	515, ^d 516, ^e 516 ^f	545.8	517.8	0	10	0.0	5.2
ν_3 (a_g)	292, ^d 291, ^e 292 ^f	258.8	271.1	0	15	0.0	2.6
ν_4 (a_g)	ca. 130 ^g	145.8	138.3	0	0	0.0	0.6
ν_5 (a_u)		329.5	312.6	0	0	0.0	0.0
ν_6 (b_{2g})	476, ^d 479, ^e 476 ^f	495.9	470.4	0	5	0.0	4.0
ν_7 (b_{2g})	ca. 180 ^h	151.2	143.5	0	0	0.0	0.1
ν_8 (b_{2u})	1450, ^d 1460, ^e obscured ^f	1508.5	1431.1	50	0	94.0	0.0
ν_9 (b_{2u})	355 ^d	372.5	353.4	15	0	18.9	0.0
ν_{10} (b_{2u})		34.3	32.5			0.5	0.0
ν_{11} (b_{1g})	1458, ^d 1467, ^e 1463 ^f	1506.3	1429.0	0	20	0.0	28.3
ν_{12} (b_{1g})	340, ^d 354, ^e 345 ^f	347.5	329.7	0	7	0.0	2.1
ν_{13} (b_{1u})	492, ^d 497, ^e 492 ^f	523.8	496.9	70	0	93.4	0.0
ν_{14} (b_{1u})	305 ^d	257.2	244.0	7	0	28.6	0.0
ν_{15} (b_{3g})	340, ^d 347, ^e 345 ^f	336.4	319.1	0	7	0.0	5.2
ν_{16} (b_{3u})	1414, ^d 1428, ^e obscured ^f	1489.1	1412.7	25	0	38.5	0.0
ν_{17} (b_{3u})	504, ^d 506, ^e 503 ^f	533.3	506.0	100	0	100.0	0.0
ν_{18} (b_{3u})	265 ^d	262.1	248.6	70	0	75.9	0.0

^a Observed spectra relate to the matrix-isolated molecule. Calculated frequencies and intensities (estimated relative to the strongest band set to 100 arbitrary units) were obtained using HF/6-311G(d). ^b Corresponding force constants scaled by 0.9. ^c Observed intensities estimated relative to the strongest band set to 100 arbitrary units. ^d Argon matrix. ^e Dinitrogen matrix. ^f Methane matrix. ^g Inferred from $2\nu_4$ at 267 cm^{-1} and ($\nu_3 + \nu_4$) at 410 cm^{-1} . ^h Inferred from ($\nu_3 + \nu_4$) at 311 cm^{-1} .

The vibrational wavenumbers listed in Table 3 differ somewhat from those proposed previously,²³ most notably in relation to the modes ν_3 , ν_6 , ν_7 , ν_{13} , ν_{15} and ν_{17} . The measured frequencies now relate exclusively to the matrix-isolated $[\text{H}_2\text{GaCl}]_2$ and $[\text{D}_2\text{GaCl}]_2$ vapors instead of being drawn in part from the liquid, the Raman spectrum of which is not reproduced entirely by the matrix-isolated species, particularly at $\tilde{\nu} < 750\text{ cm}^{-1}$. Significant frequency shifts, sometimes amounting to 50 cm^{-1} , and band-broadening imply appreciable association of the molecules in the liquid. In addition, we have altered some of the assignments previously given so as to take better account of the frequency and intensity patterns simulated here and elsewhere²⁷ by quantum chemical calculations. There is good reason therefore to believe that the present assignments reflect more closely the vibrational properties of free monochlorogall-

ane molecules; as indicated by the results included in Table 3, they are consistent with the operation of the product rule.

As usual, the vibrational wavenumbers derived from the HF/6-311G(d) calculations are generally higher than those determined experimentally. Scaling the original force constants by a factor of 0.90 gives calculated wavenumbers having a satisfactory level of agreement with the observed ones. Hence we conclude (i) that the assignments we propose here are reasonable and (ii) that the vibrational spectra are wholly consistent with a dimeric molecule $\text{H}_2\text{Ga}(\mu\text{-Cl})_2\text{GaH}_2$ conforming to D_{2h} symmetry, although a small distortion would not necessarily result in observable changes in the spectra.

(c) ¹H NMR Spectrum of Monochlorogallane. The ¹H NMR spectrum of monochlorogallane dissolved in $[\text{D}_8]\text{toluene}$ at 293 K consists of a single broad resonance at $\delta_{\text{H}} = 5.46$ (line width at half-height $W_{1/2} = 134\text{ Hz}$). The chemical shift is characteristic of hydrogen atoms forming terminal bonds to

(27) Duke, B. J.; Hamilton, T. P.; Schaefer, H. F., III. *Inorg. Chem.* **1991**, 30, 4225. Duke, B. J. Unpublished results.

Table 3. Vibrational Assignments and Product Rule Calculations for $[\text{H}_2\text{GaCl}]_2$ and $[\text{D}_2\text{GaCl}]_2^a$

irred rep	no. of mode	description	$[\text{H}_2\text{GaCl}]_2$	$[\text{D}_2\text{GaCl}]_2$	$\tilde{\nu}_\text{H}/\tilde{\nu}_\text{D}$	$\pi(\tilde{\nu}_\text{H}/\tilde{\nu}_\text{D})_i$	
			$\tilde{\nu}_\text{H}$	$\tilde{\nu}_\text{D}$		calcd	obsd
a_g	1	sym $\nu(\text{Ga}-\text{H})$	1994	1429	1.3954	1.9985	1.9415
	2	sym $\delta(\text{GaH}_2)$	719	515	1.3961		
	3	sym $\nu(\text{Ga}-\text{Cl})$	291	292	0.9966		
	4	$\nu(\text{Ga}\cdots\text{Ga})$	130	130	1.0000		
a_u	5	GaH_2 torsion	[441.9] ^b	[312.6] ^b	[1.4136] ^b	[1.4137] ^b	
b_{2g}	6	out-of-phase GaH_2 wag	656	476	1.3782	1.3901	1.3782
	7	antisym $\nu(\text{Ga}-\text{Cl})$	180	180	1.0000		
b_{2u}	8	antisym $\nu(\text{Ga}-\text{H})$	2021	1450	1.3938	1.9800	1.9773
	9	in-phase $\rho(\text{GaH}_2)$	480	355	1.3521		
	10	ring pucker	[34.1] ^b	[32.5] ^b	[1.0492] ^b		
b_{1g}	11	antisym $\nu(\text{Ga}-\text{H})$	2036	1458	1.3964	1.9601	1.9590
	12	out-of-phase $\rho(\text{GaH}_2)$	477	340	1.4029		
b_{1u}	13	in-phase GaH_2 wag	702	492	1.4268	1.4006	1.3566
	14	antisym $\nu(\text{Ga}-\text{Cl})$	290	305	0.9508		
b_{3g}	15	GaH_2 torsion	472	340	1.3882	1.3680	1.3882
b_{3u}	16	sym $\nu(\text{Ga}-\text{H})$	1998	1414	1.4130	1.9800	1.9682
	17	out-of-phase sym $\delta(\text{GaH}_2)$	702	504	1.3929		
	18	sym $\nu(\text{Ga}-\text{Cl})$	265	265	1.0000		

^a Observed frequencies (cm^{-1}) are for the molecules isolated in an argon matrix. ^b Frequency (cm^{-1}) calculated using HF/6-311G(d) and scale const = 0.9.

gallium,^{14,16,17,29–31} being at appreciably higher frequency than the shifts associated with $\text{Ga}(\mu\text{-H})_2\text{Ga}$ units.^{17,32} The broadness of the resonance is characteristic of hydrogen atoms bound to gallium (the two naturally occurring nuclei ⁶⁹Ga and ⁷¹Ga both having $I = 3/2$).

(d) Structure of Gaseous Monochlorogallane. (1) Structural Model Used in the Analysis of the Electron Diffraction Data. In light of the vibrational properties described above and in keeping with the model adopted earlier,²² the equilibrium structure of the $\text{H}_2\text{Ga}(\mu\text{-Cl})_2\text{GaH}_2$ dimer was assumed to have D_{2h} symmetry, as shown in Figure 2a. In developing a more

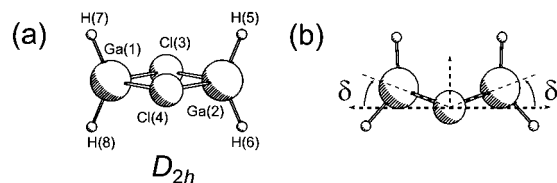


Figure 2. Representations of (a) the equilibrium structure and (b) the ring-puckering vibration of $\text{H}_2\text{Ga}(\mu\text{-Cl})_2\text{GaH}_2$.

realistic model for the analysis of the measured electron diffraction pattern, we note the very low frequency (ca. 34 cm^{-1}) predicted by theoretical calculations [HF/6-311G(d)] for the ring-puckering mode ν_{10} (b_{2u}), which consists principally of folding of the $\text{Ga}(\mu\text{-Cl})_2\text{Ga}$ ring about the $\text{Cl}\cdots\text{Cl}$ vector. In the absence of theoretical estimates at the time of the earlier analysis, the mode was assigned to what appears now to be an unrealistically high frequency (about 100 cm^{-1}) for the purposes of estimating vibrational amplitudes.^{22,33} Support for the new assignment is provided by a study of Ga_2Cl_6 where the corresponding mode occurs near 28 cm^{-1} .²⁶

To take account of the unusual flexibility of the $\text{Ga}(\mu\text{-Cl})_2\text{Ga}$ skeleton, we have adopted a dynamic model capable of

accommodating a large-amplitude motion to describe the molecular structure of $\text{H}_2\text{Ga}(\mu\text{-Cl})_2\text{GaH}_2$. The modeling has sought to represent the large-amplitude motion by a set of “pseudoconformers” distributed around the $\text{Cl}\cdots\text{Cl}$ vector such that the sum of the individual pseudoconformers reflects the molecular motion.³⁴ The individual pseudoconformers were weighted by a Boltzmann factor determined by a quartic potential $V(\delta) = V_4\delta^4 + V_2\delta^2$ [obtained by ab initio HF/6-311G(d) calculations]. Nine pseudoconformers were deployed to describe the ring puckering with intervals equal to $\Delta\delta = 5^\circ$ (see Figure 2b). The pseudoconformers were treated as distinct molecules undergoing the usual framework vibrations, except for the ring-puckering motion. The structure of each pseudoconformer was defined by modifying the parameters of the equilibrium D_{2h} form. The differences between the structural parameters of a given pseudoconformer and those of the equilibrium form were estimated by ab initio calculations, as described in the next section. The constraints were then imposed on the r_α model on the assumptions that $\Delta r_\alpha = \Delta r_e$ and that the vibrational correction is negligible.

On the basis of the HF/6-311G(d) calculations, Cartesian force constants were determined for the optimized D_{2h} molecule. By employment of the program ASYM40,²⁸ these force constants were scaled by a factor of 0.9 to generate the frequencies given in Tables 1 and 2. The scaled Cartesian force field was then converted to one described by symmetrized internal force constants, and the corresponding force field was adjusted to provide an exact fit to the observed wavenumbers. For ν_5 and ν_{10} , which were not observed, the calculated frequencies (see Tables 1 and 2) were adopted. Omitting the very low frequency ring-puckering mode (ν_{10}), we then used this force field to obtain the root-mean-square amplitudes of vibration (l), perpendicular-amplitude corrections (K), and centrifugal distortions (δr) for the molecular framework of each pseudoconformer. The resulting vibrational parameters l , K , and δr were then introduced into the refinements of the model adopted to describe the electron diffraction pattern. In the process, the vibrational amplitude l associated with a given distance in each pseudoconformer was linked to that of the D_{2h} form. Hence we have defined the structure and vibrational amplitudes of the entire system in terms of the following parameters: $r(\text{Ga}-\text{Cl})$, $r(\text{Ga}-$

(28) Hedberg, L.; Mills, I. M. *J. Mol. Spectrosc.* **1993**, *160*, 117.

(29) Beachley, O. T., Jr.; Simmons, R. G. *Inorg. Chem.* **1980**, *19*, 783. Thomas, P. D. P. D. Philos. Thesis, University of Oxford, U.K., 1977.

(30) Downs, A. J.; Harman, L. A.; Thomas, P. D. P.; Pulham, C. R. *Polyhedron* **1995**, *14*, 935.

(31) Greenwood, N. N.; Ross, E. J. F.; Storr, A. *J. Chem. Soc. A* **1966**, 706.

(32) Baxter, P. L.; Downs, A. J.; Goode, M. J.; Rankin, D. W. H.; Robertson, H. E. *J. Chem. Soc., Dalton Trans.* **1990**, 2873.

(33) Cradock, S. Unpublished results.

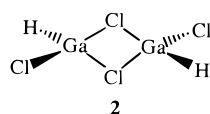
(34) Friesen, D.; Hedberg, K. *J. Am. Chem. Soc.* **1980**, *102*, 3987.

H), $\angle\text{H-Ga-H}$, $\angle\text{Cl-Ga-Cl}$, the ring-puckering angle δ , and the coefficients V_4 and V_2 for the ring-puckering potential $V(\delta)$.

(2) Refinement of the Structural Model. Least-squares analysis³⁵ of the molecular scattering intensities has been employed to refine the structure of the $\text{H}_2\text{Ga}(\mu\text{-Cl})_2\text{GaH}_2$ molecule. The geometries were calculated on the basis of r_a parameters, and these were converted to the r_a counterparts required by the scattering intensity formula. A theoretical $sI_m(s)$ curve ($s = 4\pi\lambda^{-1} \sin \theta$, where 2θ is the scattering angle) was adjusted simultaneously to the average intensity curves (derived from the different camera distances) using a unit weight matrix.

Results from preliminary refinements using the dynamic model described above gave reason to believe that the diffracted sample contained more than one compound. The main discrepancies between the experimental and theoretical radial-distribution curves appeared near 2.1 and 3.6 Å, suggesting additional scattering contributions from bonded Ga-Cl_t and nonbonded Cl_t...Cl_b atom pairs (t = terminal, b = bridging). It appears therefore that some decomposition of the monochlorogallane had occurred, a view confirmed not only by the persistent formation of an involatile residue on vaporization of the compound but also by the deposition of a white crystalline solid in the glass inlet to the diffraction chamber. Further investigations, to be described elsewhere,²¹ have shown that the crystalline solid is the mixed-valence compound $\text{Ga}^+[\text{GaCl}_3\text{H}]^-$. On this and other evidence, decomposition of monochlorogallane appears to involve disproportionation and elimination of H_2 so that possible candidates for the second component of the vapor sample are another molecule of the type $\text{Ga}_2\text{Cl}_6\text{H}_{6-x}$ where $x > 2$ or a hydrogen-loss product like GaGaCl_4 ³⁶ or GaGaCl_3H .

Subsequent refinements were therefore attempted on the basis of models consisting mainly of $\text{H}_2\text{Ga}(\mu\text{-Cl})_2\text{GaH}_2$ with the admixture of small but variable proportions of each of the digallium species *cis*- and *trans*- $\text{H}(\text{Cl})\text{Ga}(\mu\text{-Cl})_2\text{Ga}(\text{Cl})\text{H}$,^{27,29} $\text{H}_2\text{Ga}(\mu\text{-Cl})_2\text{GaCl}_2$, $\text{H}_2\text{Ga}(\mu\text{-Cl})_2\text{Ga}(\text{Cl})\text{H}$, Ga_2Cl_6 ,³⁷ $\text{Ga}(\mu\text{-Cl})_2\text{-GaCl}_2$,³⁶ and $\text{Ga}(\mu\text{-Cl})_2\text{Ga}(\text{Cl})\text{H}$. The best account of the measured scattering, with a simultaneous lowering of the *R* factor, was achieved with a model comprising a mixture of $\text{H}_2\text{Ga}(\mu\text{-Cl})_2\text{GaH}_2$ and *trans*- $\text{H}(\text{Cl})\text{Ga}(\mu\text{-Cl})_2\text{Ga}(\text{Cl})\text{H}$, **2**. However,



the improvement was not sufficient to eliminate conclusively the presence of *cis*- $\text{H}(\text{Cl})\text{Ga}(\mu\text{-Cl})_2\text{Ga}(\text{Cl})\text{H}$, $\text{H}_2\text{Ga}(\mu\text{-Cl})_2\text{Ga}(\text{Cl})\text{H}$, or Ga_2Cl_6 as the secondary component.

Consideration of the properties of the various compounds lends weight to the conclusion that *trans*- $\text{H}(\text{Cl})\text{Ga}(\mu\text{-Cl})_2\text{Ga}(\text{Cl})\text{H}$ is the species most likely to be present under the conditions of our experiments. This is a known compound, decomposition of which is reported²⁴ to occur at temperatures above its melting point (302 K) and to be complete at 423 K. According to quantum chemical calculations,²⁷ *trans*- $\text{H}(\text{Cl})\text{Ga}(\mu\text{-Cl})_2\text{Ga}(\text{Cl})\text{H}$ is predicted to be marginally more stable than the *cis* isomer. The gallium(III) chloride dimer, Ga_2Cl_6 ,³⁷ is a familiar, stable molecule at 320 K or higher temperatures but has not been detected as a decomposition product of monochlo-

rogallane. Neither GaGaCl_4 (on the evidence of earlier experiments³⁶) nor GaGaCl_3H (on the evidence of our studies²¹) appears to be volatile enough to have a significant presence in the vapor at 320 K. Hence we conclude that our model, consisting of a mixture of $\text{H}_2\text{Ga}(\mu\text{-Cl})_2\text{GaH}_2$ and *trans*- $\text{H}(\text{Cl})\text{Ga}(\mu\text{-Cl})_2\text{Ga}(\text{Cl})\text{H}$, provides the most plausible basis for interpreting the measured electron diffraction pattern. Structure parameters for *trans*- $\text{H}(\text{Cl})\text{Ga}(\mu\text{-Cl})_2\text{Ga}(\text{Cl})\text{H}$ were tied to the analogous parameters of $\text{H}_2\text{Ga}(\mu\text{-Cl})_2\text{GaH}_2$, with differences constrained at the values derived from the ab initio calculations [MP2 level of theory with all electrons included in the correlation calculations and a 6-311G(d) basis set]. The Ga-Cl_t distance in *trans*- $\text{H}(\text{Cl})\text{Ga}(\mu\text{-Cl})_2\text{Ga}(\text{Cl})\text{H}$ was tied to the Ga-Cl_b distance in $\text{H}_2\text{Ga}(\mu\text{-Cl})_2\text{GaH}_2$.

The refinement calculations failed to bring about convergence of the H-Ga-H angle and the coefficients for the ring-puckering potential, which were therefore constrained at the values given by the ab initio calculations [MP2/6-311G(d)]; reasonable variations in these parameters had little or no effect on the structure parameters that were amenable to refinement. The value of 135.1° thus associated with $\angle\text{H-Ga-H}$ is somewhat larger than that adopted in the earlier analysis²² but consistent with the results of various quantum chemical calculations performed on molecules containing an $\text{H}_2\text{Ga}(\mu\text{-X})_2$ structural unit (cf. 129.9° in Ga_2H_6 ,³⁸ 130.0° in $\text{H}_2\text{Ga}(\mu\text{-H})_2\text{BH}_2$,³⁹ and 131.0° in $\text{H}_2\text{Ga}(\mu\text{-H})_2\text{B}_3\text{H}_6$ ¹⁷). The proportion of *trans*- $\text{H}(\text{Cl})\text{Ga}(\mu\text{-Cl})_2\text{Ga}(\text{Cl})\text{H}$ present in the vapor was typically about 9%, and a check was made to ensure that the final structure parameters determined for $\text{H}_2\text{Ga}(\mu\text{-Cl})_2\text{GaH}_2$ were not significantly affected by changes in this proportion or in the parameters defining the minor component.

Results from the refinements are given in Table 4. Values for the experimental distances and bond angles are averages over all pseudoconformers, each pseudoconformer being Boltzmann-weighted according to the calculated puckering potential. All the experimental amplitudes are similarly weight-averaged values. Intensity curves calculated for the final model are shown in Figure 3, together with the experimental and difference curves. Figure 4 shows the corresponding radial distribution curves. Although all uncertainties are quoted as 1σ values, the difficult nature of the refinement and the additional complication of the presence of a second component make it more realistic to consider 2σ or even 3σ as a measure of the uncertainty in the value of a given parameter. The best defined parameters are the Ga-H distance (corresponding to the peak near 1.5 Å) and the Ga-Cl distance (identifiable with the prominent feature near 2.3 Å); the Ga...Ga and Cl...Cl nonbonded distances together account for the only other major peak (centered near 3.3 Å). The correlation matrix for the refined parameters is given in Table 5. The final *R* factor (*R*_G) was 0.115.

The present estimate of 1.523(20) Å for $r_a(\text{Ga-H})$ [$r_a = 1.542(20)$ Å] is in accord with the most recent values determined for other molecules incorporating terminal Ga-H bonds, e.g. $\text{HGa}(\text{BH}_4)_2$ [$r_a(\text{Ga-H}) = 1.49(4)$ Å]⁴⁰ and $\text{H}_2\text{GaB}_3\text{H}_8$ [$r_a(\text{Ga-H}) = 1.493(14)$ Å].¹⁷ It is not significantly different from the corresponding distance in the gallane complex $\text{Me}_3\text{N}\cdot\text{GaH}_3$ [$r_a(\text{Ga-H}) = 1.511(13)$ Å],⁴¹ although the $\nu(\text{Ga-H})$ modes,

(35) Hedberg, K.; Iwasaki, M. *Acta Crystallogr.* **1964**, *17*, 529.

(36) Giricheva, N. I.; Girichev, G. V.; Titov, V. A.; Chusova, T. P.; Pavlova, G. Yu. *Zh. Strukt. Khim.* **1992**, *33*, 50.

(37) Shen, Q. Ph.D. Thesis, Oregon State University, 1974. Petrov, V. M.; Giricheva, N. I.; Girichev, G. V.; Titov, V. A.; Chusova, T. P. *Zh. Strukt. Khim.* **1991**, *32*, 56.

(38) See, for example: Shen, M.; Schaefer, H. F., III. *J. Chem. Phys.* **1992**, *96*, 2868. Barone, V.; Orlandini, L.; Adamo, C. *J. Phys. Chem.* **1994**, *98*, 13185.

(39) van der Woerd, M. J.; Lammertsma, K.; Duke, B. J.; Schaefer, H. F., III. *J. Chem. Phys.* **1991**, *95*, 1160.

(40) Downs, A. J.; Greene, T. M.; Harman, L. A.; Souter, P. F.; Brain, P. T.; Pulham, C. R.; Rankin, D. W. H.; Robertson, H. E.; Hofmann, M.; Schleyer, P. v. R. *Inorg. Chem.* **1995**, *34*, 1799.

Table 4. Structural Parameters for $\text{H}_2\text{Ga}(\mu\text{-Cl})_2\text{GaH}_2$

param ^a	electron diffraction	ab initio ^b	param ^a	electron diffraction	ab initio ^b
	$r_{\alpha}/\angle_{\alpha}$	r_e/\angle_e		$r_{\alpha}/\angle_{\alpha}$	r_e/\angle_e
$r(\text{Ga}-\text{Cl})$	2.350(2)	2.369	V_4	$[3 \times 10^{-6}]^c$	$3 \times 10^{-6}^c$
$r(\text{Ga}-\text{H})$	1.523(20)	1.546	V_2	$[6 \times 10^{-4}]^c$	$6 \times 10^{-4}^c$
$\angle\text{ClGaCl}$	89.7(5)	89.0	$M_{\text{F}}(\text{Ga}_2\text{Cl}_2\text{H}_4)$	91(3) ^d	
$\angle\text{HGaH}$	[135.1]	135.1			

param ^a	electron diffraction				ab initio	
	r_{g}^e	r_{α}^e	r_{e}^e	l_{expt}	r_{e}^b	l_{calcd}^f
$r(\text{Ga}-\text{Cl})$	2.352(2)	2.349(2)	2.349(2)	0.087(3)	2.369	0.079
$r(\text{Ga}-\text{H})$	1.547(20)	1.542(20)	1.523(20)	[0.092]	1.546	0.092
$r(\text{Ga}\cdots\text{Ga})$	3.290(14)	3.287(14)	3.286(14)	0.099(5)	3.380	0.106
$r(\text{Cl}_3\cdots\text{Cl}_4)$	3.302(16)	3.300(16)	3.300(16)	0.092(5)	3.320	0.097
$r(\text{Cl}_3\cdots\text{H}_5)$	3.139(14)	3.131(14)	3.128(14)	[0.160]	3.162	0.160
$r(\text{Ga}_1\cdots\text{H}_7)$	4.112(18)	4.104(18)	4.103(18)	[0.179]	4.220	0.179

^a Distances (r) and amplitudes (l) are in Å and angles (\angle) are in deg. Parenthesized values are σ and include estimates of uncertainties in voltage/nozzle height and of correlation in experimental data. The data given are for $\text{H}_2\text{Ga}(\mu\text{-Cl})_2\text{GaH}_2$ with D_{2h} symmetry. Values in square brackets are constrained at the calculated values. ^b MP2 level of theory with all the electrons included in the correlation calculation and a 6-311G(d) basis set. ^c $V = V_4\delta^4 + V_2\delta^2$; δ in deg, V_4 in kcal mol⁻¹ deg⁻⁴, and V_2 in kcal mol⁻¹ deg⁻². ^d Mole fraction (%) of $\text{Ga}_2\text{Cl}_2\text{H}_4$ in vapor sample. ^e Average distances over all the pseudoconformers. ^f Calculated from the force field that gives an exact fit to the observed frequencies.

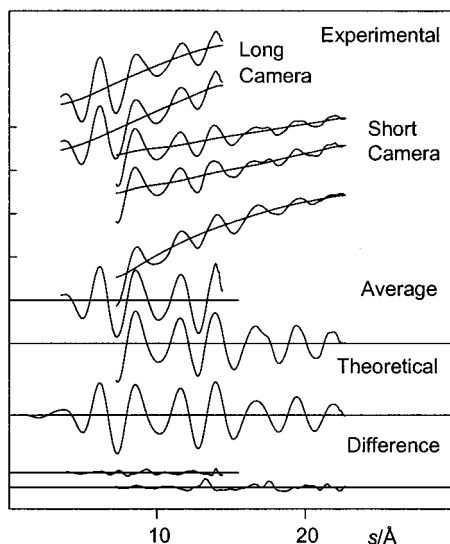


Figure 3. Experimental molecular-scattering curves [$s^4I(s)$] for $\text{H}_2\text{Ga}(\mu\text{-Cl})_2\text{GaH}_2$. The results are shown magnified 7-fold with respect to the final backgrounds on which they are superimposed. The average curves are $sI_m(s) = s(s^4I - \text{background})$.

being some 100 cm⁻¹ lower for the complex than for the base-free $\text{H}_2\text{Ga}(\mu\text{-Cl})_2\text{GaH}_2$ molecule, imply that it is actually somewhat shorter in the latter. The present study thus underlines the difficulties of placing Ga-H bond lengths on an accurate quantitative scale.^{2,41} Much better defined is the distance r_a -(Ga-Cl), which at 2.349(2) Å is intermediate between the corresponding parameters for Ga_2Cl_6 [$r_a = 2.300(1)$ Å]³⁷ and $\text{Me}_2\text{Ga}(\mu\text{-Cl})_2\text{GaMe}_2$ [$r_a = 2.378(4)$ Å]³² (see Table 6).

The calculated vibrational amplitudes showed little dependence on the precise force field used, irrespective of whether it came from ab initio or experimental sources or of whether the ab initio field was scaled or unscaled. Where comparisons could be made, these calculated amplitudes agreed with the refined amplitudes derived from the GED pattern, at least within the limits of uncertainty associated with the latter estimates.

(3) Theoretical Calculations. It is now common to carry out ab initio calculations to aid the analysis of electron

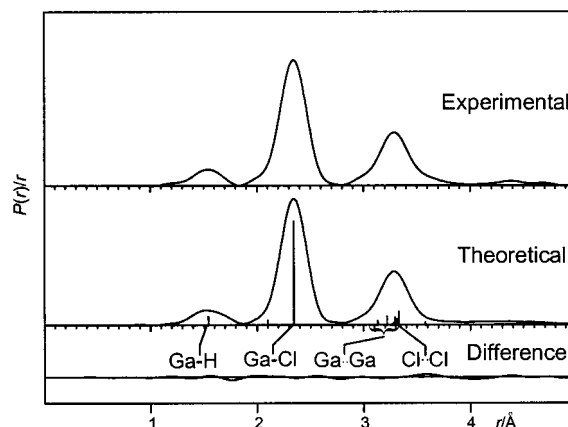


Figure 4. Radial distribution curves for $\text{H}_2\text{Ga}(\mu\text{-Cl})_2\text{GaH}_2$ [91(3)%] admixed with some *trans*- $\text{HClGa}(\mu\text{-Cl})_2\text{GaHCl}$ [9(3)%]. The experimental curve was calculated from the composite of the two average intensity curves with the use of theoretical data for the region $0 \leq s \leq 3.00 \text{ Å}^{-1}$ with a damping factor of 0.0025 Å^2 . The difference curve represents the experimental minus the theoretical curve. The vertical lines indicate important interatomic distances, and each has a height proportional to the weight of the distance.

Table 5. Correlation Matrix ($\times 100$) for Parameters Refined in the Final Least Squares Calculations for $\text{H}_2\text{Ga}(\mu\text{-Cl})_2\text{GaH}_2^a$

no.	param	σ_{LS}^b	r_1	r_2	\angle_3	l_4	l_5	M_{F_6}
1	$r_1(\text{Ga}-\text{Cl})$	0.0012	100	6	45	-15	6	-42
2	$r_2(\text{Ga}-\text{H})$	0.0139		100	5	-13	5	-5
3	$\angle_3\text{ClGaCl}$	0.3481			100	-12	-10	-14
4	$l_4(\text{Ga}_1-\text{Cl}_3)$	0.0015				100	21	24
5	$l_5(\text{Ga}_1\cdots\text{Ga}_2)$	0.0028					100	-25
6	$M_{F_6}(\text{Ga}_2\text{Cl}_2\text{H}_4)$	0.0170						100

^a Distances (r) and amplitudes (l) are in Å and angles (\angle) are in deg. ^b Standard deviation from least-squares refinement.

diffraction data, and this procedure we have followed for the results described above. One of the major decisions that has then to be taken concerns the selection of an appropriate modulus operandi. The results of the theoretical calculations on $\text{H}_2\text{Ga}(\mu\text{-Cl})_2\text{GaH}_2$, at different levels of theory and with different numbers of polarization and diffuse functions on the 6-311G basis set, are presented in Table 7. Hence it is evident that the absolute values calculated for the structure parameters do not vary greatly with the number of polarization and diffuse functions added to the 6-311G basis set at a given level of theory

(41) Brain, P. T.; Brown, H. E.; Downs, A. J.; Greene, T. M.; Johnsen, E.; Parsons, S.; Rankin, D. W. H.; Smart, B. A.; Tang, C. Y. *J. Chem. Soc., Dalton Trans.* **1998**, 3685.

Table 6. Comparison of Structural Parameters for $\text{H}_2\text{Ga}(\mu\text{-Cl})_2\text{GaH}_2$ with Those for Related Molecules

parameter ^a	$\text{H}_2\text{Ga}(\mu\text{-Cl})_2\text{GaH}_2$		$\text{Me}_2\text{Ga}(\mu\text{-Cl})_2\text{GaMe}_2$	$\text{Cl}_2\text{Ga}(\mu\text{-Cl})_2\text{GaCl}_2$	$\text{H}_2\text{Ga}(\mu\text{-H})_2\text{GaH}_2$	$\text{MeClGa}(\mu\text{-Cl})_2\text{GaClMe}$
$r(\text{Ga}-\text{Cl}_b)$	2.349(2)	2.349(3)	2.378(4)	2.300(1)		2.339(3)
$r(\text{Ga}-\text{X}_i)$	1.542(20)	1.559(19)	1.946(3)	2.099(1)	1.519(35)	2.129(3) ^b
$r(\text{Ga}\cdots\text{Ga})$	3.287(14)	3.241(7)	3.303(19)	3.301(12)	2.580(2)	3.297(15)
$\angle\text{Cl}_b\text{GaCl}_b$	89.2(5) ^c	92.8(8)	92.0(9)	88.4(4)		90.4(6)
$\angle\text{X}_i\text{GaX}_i$	135.1 ^{c,d}	120 ^d	132.1(27)	124.6(9)	130.0 ^d	131(3)
$l(\text{Ga}-\text{X}_i)$	0.087(3)	0.071(3)	0.093(2)		0.120(51)	0.085(2)
$l(\text{Ga}-\text{X}_i)$	0.092 ^d	0.092 ^d	0.059(5)		0.100(51)	0.056(2) ^b
$l(\text{Ga}\cdots\text{Ga})$	0.099(5)	0.086(7)	0.100(10)		0.065(4)	0.107(4)
source	this work	ref 22	ref 32	ref 37	ref 14	ref 42

^a Distances (r_a) and amplitudes (l) are in Å, and angles (\angle) are in deg; X = H, C, Cl, or a combination of these. ^b Value for $r(\text{Ga}-\text{Cl}_i)$. ^c r_a angles quoted for comparison only. ^d Assumed.

Table 7. Results from the ab Initio Calculations on $\text{H}_2\text{Ga}(\mu\text{-Cl})_2\text{GaH}_2$ and *trans*- $\text{ClHGa}(\mu\text{-Cl})_2\text{GaClH}$

$\text{H}_2\text{Ga}(\mu\text{-Cl})_2\text{GaH}_2$									
calculation	parameter ^a								energy, hartrees
HF/6-311G(d)	D_{2h}	Ga-Cl	Ga-H ₅	Ga-H ₆	HGaH	ClGaH ₅	ClGaH ₆	ClGaCl	GaClGa
	$\delta = 5$	2.4052	1.5525	1.5525	133.20	106.66	106.66	87.57	92.43
	$\delta = 10$	2.4052	1.5527	1.5522	133.28	106.45	106.83	87.52	92.03
	$\delta = 15$	2.4054	1.5529	1.5519	133.37	106.26	107.05	87.23	90.95
	$\delta = 20$	2.4061	1.5530	1.5516	133.50	106.04	107.31	86.75	89.19
HF/6-311G(d,p)	D_{2h}	2.4088	1.5527	1.5513	133.67	105.91	107.53	85.97	86.85
	$\delta = 5$	2.4069	1.5497	1.5497	133.32	106.62	106.62	87.59	92.41
	$\delta = 10$	2.4070	1.5499	1.5494	133.32	106.41	106.86	87.46	92.09
	$\delta = 15$	2.4064	1.5502	1.5492	133.36	106.26	107.05	87.23	90.96
	$\delta = 20$	2.4077	1.5501	1.5488	133.53	106.03	107.29	86.75	89.19
HF/6-311+G(d)	D_{2h}	2.4099	1.5500	1.5485	133.71	105.91	107.51	85.96	86.86
HF/6-311+G(d,p)	D_{2h}	2.4062	1.5530	1.5530	133.09	106.67	106.67	87.77	92.24
HF/6-311++G(d)	D_{2h}	2.4079	1.5501	1.5501	133.17	106.65	106.65	87.73	92.27
HF/6-311++G(d,p)	D_{2h}	2.4061	1.5530	1.5530	133.06	106.68	106.68	87.76	92.25
MP2/6-311G(d) ^b	D_{2h}	2.4070	1.5502	1.5502	133.04	106.69	106.69	87.75	92.25
MP2/6-311G(d) ^c	D_{2h}	2.3951	1.5615	1.5615	134.94	105.94	105.94	88.41	91.60
MP2/6-311G(d) ^d	D_{2h}	2.3688	1.5444	1.5444	135.08	105.83	105.83	88.88	91.12
	$\delta = 5$	2.3690	1.5462	1.5462	135.10	105.81	105.81	88.97	91.03
	$\delta = 10$	2.3687	1.5466	1.5459	135.06	105.62	106.05	88.88	90.68
	$\delta = 15$	2.3684	1.5469	1.5456	135.09	105.40	106.32	88.63	89.61
	$\delta = 20$	2.3684	1.5471	1.5453	135.15	105.17	106.63	88.19	87.85
MP2/6-311G(d,p) ^d	D_{2h}	2.3695	1.5469	1.5451	135.22	105.05	106.89	87.49	85.51
MP2/6-311+G(d) ^d	D_{2h}	2.3656	1.5304	1.5304	134.77	105.93	105.93	88.95	91.05
MP2/6-311+G(d,p) ^d	D_{2h}	2.3706	1.5465	1.5465	134.90	105.89	105.89	88.87	91.13
MP2/6-311++G(d,p) ^d	D_{2h}	2.3669	1.5309	1.5309	134.43	106.05	106.05	88.87	91.13
MP2/6-311++G(d,p) ^d	D_{2h}	2.3706	1.5465	1.5465	134.90	105.89	105.89	88.87	91.13
MP2/6-311++G(d,p) ^d	D_{2h}	2.3668	1.5308	1.5308	134.41	106.06	106.06	88.88	91.13
MP3/6-311G(d) ^b	D_{2h}	2.3996	1.5660	1.5660	135.19	105.88	105.88	88.27	91.73

<i>trans</i> - $\text{ClHGa}(\mu\text{-Cl})_2\text{GaClH}$									
calculation	parameter ^a							energy, hartrees	
MP2/6-311G(d) ^d	Ga-Cl _b	Ga-Cl _i	Ga-H	Cl _b GaH	Cl _b GaCl _i	Cl _b GaCl _b	GaCl _b Ga	-5687.539 726 29	
	2.3396	2.1241	1.5391	128.67	106.11	89.28	90.72		

^a Distances are in Å, and angles are in degrees. ^b All the core electrons were excluded from the correlation calculations. ^c The Ga 3d electrons were included in the correlation calculations. ^d All the electrons were included in the correlation calculations.

but that larger variations arise when different levels of theory are employed. Of particular interest is the Ga-Cl bond distance, which decreases from 2.405 to 2.369 Å with the change in the level of theory from HF to MP2 (with all the electrons included in the correlation calculation), 6-311G(d) being the basis set used. The distances estimated in the MP2 calculations are dependent on which orbitals are included in the correlation calculation. If a frozen core (all the core electrons excluded from the correlation calculation) is assumed, $r(\text{Ga}-\text{Cl})$ is calculated to be 2.395 Å. If the Ga 3d orbitals are included or if all orbitals are included in the correlation calculation, however, the distance is calculated as 2.369 Å. We believe that as the Ga 3d orbitals are close in energy to the valence 4s orbital, it is important to include them in the correlation calculation. The MP3 level of theory (with all the core electrons excluded from the correlation

calculation) gives a Ga-Cl distance similar to the one computed at the MP2 level. The ring-puckering potential is predicted to be slightly wider by the MP2 than by the HF calculations. With the basis sets used to date, calculations here and elsewhere^{27,38,40,41} yield bond distances that are in general longer than the experimentally determined ones. For $\text{H}_2\text{Ga}(\mu\text{-Cl})_2\text{GaH}_2$, the MP2 level of theory [with all the core electrons included in the correlation calculation and a 6-311G(d) basis set] comes closer to replicating the experimental dimensions than do the following: HF, MP2, and MP3 (with all the core electrons excluded from the correlation calculation).

Experimental Section

(a) **Synthesis of Monochlorogallane.** Monochlorogallane was prepared by the reaction between gallium(III) chloride (either supplied

Table 8. Experimental Conditions in the Electron Diffraction Study of $\text{H}_2\text{Ga}(\mu\text{-Cl})_2\text{GaH}_2$

nozzle to plate dist, cm	wavelength, Å	temp of sample, °C	temp of nozzle, °C	no. of plates used
19.843	0.056 86	45	50	1
24.383	0.058 78	50	50–58	2
49.425	0.058 79	45–50	56	2

by Aldrich with a quoted purity of 99.99% or prepared by direct reaction of the elements and purified by repeated vacuum sublimation) and trimethylsilane, itself made by the reduction of Me_3SiCl (Aldrich) with LiAlH_4 (Aldrich) in dried dioxane.⁴³ This took place at 250 K (eq 4) under rigorously solvent- and grease-free conditions.² In a typical experiment, powdered gallium(III) chloride (500 mg, 2.8 mmol GaCl_3) reacted with Me_3SiH (1.5 g, 20 mmol) in the space of 7 h. Following removal of any noncondensable gas, the excess of Me_3SiH and most of the Me_3SiCl coproduct were allowed to evaporate in vacuo from the reaction mixture held at 210 K. The remaining mixture was warmed to ca. 258 K, and the components volatile at this temperature were fractionated among traps held at 273, 228, and 77 K. Monochlorogallane (250 mg, 2.3 mmol of H_2GaCl) collected slowly in the 228 K trap as a colorless, viscous liquid. A small quantity of involatile white solid remained in the reaction vessel and in the 273 K trap, while the most volatile fraction (collecting in the 77 K trap) included traces of a labile gallium-containing compound (possibly gallane¹⁴).

The authenticity of a sample of monochlorogallane can be checked by reference to its vaporization properties, the IR spectrum of the solid condensate formed at 77 K,²³ and the ^1H NMR spectrum of the compound in $[\text{D}_8]\text{toluene}$ solution at temperatures in the range 193–293 K. Such a sample was stored at 77 K in a sealed, evacuated all-glass ampule equipped with a break-seal, until required. The synthesis of the deuterated derivative, $[\text{D}_2\text{GaCl}]_2$, from Me_3SiD followed similar lines.

(b) Spectroscopic Measurements and Analysis. IR spectra were recorded using one of three spectrometers, viz. a Perkin-Elmer model 580 dispersive ($4000\text{--}200\text{ cm}^{-1}$), a Mattson Polaris FT-IR ($4000\text{--}400\text{ cm}^{-1}$), or a Mattson Galaxy FT-IR instrument ($4000\text{--}400\text{ cm}^{-1}$). Raman spectra were excited at $\lambda = 514.5\text{ nm}$ with a Spectra-Physics model 165 Ar^+ laser and measured with a Spex Ramalog 5 spectrophotometer operated with a computerized data-handling center; the resolution was normally 2 cm^{-1} . Solid argon, nitrogen, and methane matrixes, typically at dilutions of gallane:matrix gas = ca. 1:200, were prepared by continuous codeposition of the gallane vapor with an excess of the matrix gas on a CsI window cooled to 15–20 K by means of a Displex refrigerator (Air Products model CS 202); fuller details of the relevant equipment and procedures are given elsewhere.^{44,45}

^1H NMR measurements on $[\text{D}_8]\text{toluene}$ solutions at temperatures between 193 and 293 K were made at 250, 300, or 500 MHz using a Bruker AM250, a Bruker AM300, or a Varian UNITY-plus 500 instrument, respectively.

(c) Electron Diffraction Measurements. Electron diffraction measurements were made using (i) an all-glass nozzle with the Reading gas diffraction apparatus⁴⁶ or (ii) a metal inlet accessed via a stainless steel needle valve with the Edinburgh apparatus.^{22,47} The monochlorogallane sample was held at a temperature between 43 and 50 °C, and the nozzle temperature was held between 48 and 58 °C. Initial attempts to measure the electron diffraction pattern were hampered by extreme fogging of the photographic (Kodak Electron Image) plates. This problem was alleviated in the studies made at Reading by extending the cold trap of the apparatus so that it enveloped the nozzle, thereby reducing the amount of vapor coming into contact with the photographic emulsion and simultaneously decreasing the pressure in the chamber. Several sets of measurements were made with varying degrees of success. Careful analysis to determine which of the results offered the best signal-to-noise ratio led to the selection of two sets of measurements at a camera distance of ca. 50 cm (both made at Reading) and three sets of measurements at a camera distance of 20–25 cm (one made at ca. 20 cm at Edinburgh, two made at 25 cm at Reading), the relevant conditions being specified in Table 8. The electron wavelength was determined immediately prior to each experiment by calibration

with the electron diffraction pattern of benzene vapor.⁴⁸ Before any measurements were made on the gallane vapor, the inlet system was conditioned by exposing it to a slow stream of the vapor for ca. 2 min. The exposed plates were left under pumping, typically for 24 h, before being developed. Tracing of the plates was then carried out with the aid either of a computer-controlled Joyce-Loebl MDM6 microdensitometer at Daresbury⁴⁹ or of the scanner in the Chemistry Department at the University of Oslo.⁵⁰ The results spanning the ranges $3.5 = s = 14.5\text{ Å}^{-1}$ and $7.25 = s = 22.75\text{ Å}^{-1}$ at intervals of $\Delta s = 0.25\text{ Å}^{-1}$ were processed by the methods described previously⁵¹ using the scattering factors taken from ref 52.

(d) Theoretical Calculations. Ab initio calculations involving the program GAUSSIAN 94⁵³ were carried out for selected pseudoconformers of the molecule $\text{H}_2\text{Ga}(\mu\text{-Cl})_2\text{GaH}_2$ to determine the structure parameters required to set up the different pseudoconformers in the theoretical model. The calculations included complete structure optimization over the range $0 = \delta = 20^\circ$ at intervals of 5° at the HF/6-311G(d), HF/6-311G(d,p), and MP2/6-311G(d) levels (with all the electrons included in the correlation calculation). In addition, calculations with different numbers of polarization and diffuse functions and levels of theory were performed for the equilibrium D_{2h} form of the $[\text{H}_2\text{GaCl}]_2$ molecule to examine the effects on the structure parameters; the relevant details of these calculations are included in Table 7. The results from geometry optimization at the MP2/6-311G(d) level (with all the electrons included in the correlation calculation) were incorporated into the theoretical model adopted for the detailed analysis of the GED results.

Acknowledgment. We thank (i) the EPSRC for research studentships (to E.J. and P.F.S.), an advanced fellowship (to T.M.G.), and other financial support of the Oxford group and also for financial support of the Edinburgh Electron Diffraction Service (Grant GR/K44411), (ii) the Norwegian Research Council (NFR) for a postdoctoral grant (to K.A.), (iii) the Norwegian National Supercomputer Committee (TRU) for a grant of computing time on the Cray J90 and Cray T3E, and (iv) Professor A. Haaland and Mrs. S. Gundersen for providing the electron scattering intensity data from the photographic plates.

Supporting Information Available: Tables of symmetry coordinates, force constants, and Cartesian coordinates for $\text{H}_2\text{Ga}(\mu\text{-Cl})_2\text{GaH}_2$. This material is available free of charge via the Internet at <http://pubs.acs.org>.

IC9908975

- (42) Akobiya, M. M.; Bregadze, V. I.; Golubinskaya, L. M.; Gundersen, S.; Haaland, A.; Volden, H. V.; Mastryukov, V. S.; Shishkov, I. F. *J. Organomet. Chem.* **1994**, *467*, 161.
- (43) Finholt, A. E.; Bond, A. C., Jr.; Wilzbach, K. E.; Schlesinger, H. I. *J. Am. Chem. Soc.* **1947**, *69*, 2692.
- (44) See, for example: Hawkins, M.; Downs, A. J. *J. Phys. Chem.* **1984**, *88*, 1527, 3042.
- (45) Souter, P. F.; Andrews, L.; Downs, A. J.; Greene, T. M.; Ma, B.; Schaefer, H. F., III. *J. Phys. Chem.* **1994**, *98*, 12824.
- (46) Holwill, C. J. Ph.D. Thesis, University of Reading, U.K., 1987.
- (47) Pulham, C. R. D.Phil. Thesis, University of Oxford, U.K., 1991.
- (48) Tamagawa, K.; Iijima, T.; Kimura, M. *J. Mol. Struct.* **1976**, *30*, 243.
- (49) Cradock, S.; Koprowski, J.; Rankin, D. W. H. *J. Mol. Struct.* **1981**, *77*, 113.
- (50) Gundersen, S.; Strand, T. G. *J. Appl. Crystallogr.* **1996**, *29*, 638.
- (51) Hagen, K.; Hobson, R. J.; Holwill, C. J.; Rice, D. A. *Inorg. Chem.* **1986**, *25*, 3659.
- (52) Ross, A. W.; Fink, M.; Hilderbrandt, R. In *International Tables for Crystallography*; Wilson, A. J. C., Ed.; Kluwer Academic Publishers: Dordrecht, The Netherlands, 1992; Vol. C, p 245.
- (53) Frisch, M. J.; Trucks, G. W.; Schlegel, H. B.; Gill, P. M. W.; Johnson, B. G.; Robb, M. A.; Cheeseman, J. R.; Keith, T.; Petersson, G. A.; Montgomery, J. A.; Raghavachari, K.; Al-Laham, M. A.; Zakrzewski, V. G.; Ortiz, J. V.; Foresman, J. B.; Cioslowski, J.; Stefanov, B. B.; Nanayakkara, A.; Challacombe, M.; Peng, C. Y.; Ayala, P. Y.; Chen, W.; Wong, M. W.; Andres, J. L.; Replogle, E. S.; Gomperts, R.; Martin, R. L.; Fox, D. J.; Binkley, J. S.; Defrees, D. J.; Baker, J.; Stewart, J. P.; Head-Gordon, M.; Gonzalez, C.; Pople, J. A. *GAUSSIAN 94*, Revision D.4; Gaussian, Inc.: Pittsburgh, PA, 1995.